Cusp Ion Composition as an Indicator of Non-Steady Reconnection

S. A. Fuselier and K. J. Trattner

Lockheed Martin Advanced Technology Center

In situ cusp observations provide a snapshot of magnetopause conditions. For southward IMF, these observations often indicate that reconnection at the magnetopause is occurring in a non-steady manner. The signature for this variability is nearly discontinuous changes in the low energy cutoff of the magnetosheath ions in the cusp. Often this low energy cutoff is difficult to observe. Recently, another indicator for this non-steady reconnection has been identified. Using composition measurements from the POLAR spacecraft, it has been shown that the differences in the magnetosheath velocity distributions leads to a distinctive, relatively slow variation in the solar wind ion composition through the cusp. More rapid changes in this cusp composition indicate changes in reconnection at the magnetopause. All southward IMF cusp intervals sampled here showed these rapid changes in the cusp ion composition. The average period of these oscillations was approximately 2 minutes. These oscillations are consistent with ~20% variations in the reconnection rate and/or the deHoffmann-Teller velocity at the magnetopause.

1. INTRODUCTION

The understanding of the transfer of mass, momentum, and energy from the solar wind into the magnetosphere is an important problem in magnetospheric physics. Spacecraft observations at the Earth's magnetopause [e.g., *Sonnerup et al.,* 1981] have confirmed the prediction by *Dungey* [1961] that this transfer can occur through magnetic reconnection of magnetosheath and magnetospheric field lines. Quantifying the transfer through this process is a more difficult problem. It requires knowledge of the reconnection rate and the spatial extent over which this reconnection is occurring, two quantities that are not easily obtained at the magnetopause. Most in situ observations can be readily related to reconnection as a mechanism for plasma transfer across the magnetopause but few observations relate to its rate. One exception is the magnitude of the normal component of the magnetic field at the magnetopause. However, this component is not easily observed [e.g., *Sonnerup and Ledley,* 1979]. Determining the spatial extent over which reconnection is occurring is very difficult because it requires determining the rate over the entire magnetopause.

Quantifying the transfer of mass, momentum, and energy across the magnetopause through reconnection is further complicated by the fact that reconnection is not steady. Changing conditions in the magnetosheath cause the reconnection x-line (or lines) to move, the field line convection to change, and the reconnection

rate to vary. Long term variations in the location of reconnection (and to a lesser extent in the rate of reconnection) have been investigated using statistical methods [e.g., *Phan et al.,* 1996]. Shorter term variations in reconnection (i.e., of the order of minutes) are not easily addressed with in situ observations at the magnetopause.

Magnetospheric field lines at the magnetopause converge in the Earth's cusps. For some time, it has been recognized that the cusp is an excellent place to monitor changes at the magnetopause in general and changes in reconnection in particular [e.g., *Lockwood and Smith,* 1992]. This is especially true for southward IMF, where subsolar reconnection produces a relatively simple cusp geometry [e.g., *Rosenbauer et al.,* 1975; *Reiff et al.,* 1977]. In this geometry, the low latitude boundary layer, cusp proper, and mantle [e.g., *Newell and Meng,* 1992] are considered a single region, called the cusp. Poleward convection of reconnected magnetic field lines produces a velocity filter effect of the precipitating magnetosheath plasma. For low altitude spacecraft such DMSP, the spacecraft velocity is rapid compared to this field line convection velocity and a traversal of the cusp yields a snapshot of nearly the entire dayside magnetopause at an "instant" in time. For high altitude spacecraft such as POLAR, the spacecraft velocity can be smaller than the field line convection velocity and the spacecraft can "monitor" a region of the magnetopause at a given location within the cusp for some time.

Relatively simple models of this ion precipitation under southward IMF conditions have been developed and tested. These models have been very successful in reproducing important features of the cusp [e.g., *Lockwood and Smith,* 1992; *Onsager et al.,* 1993].

Specifically, there are observations of energy-latitude dispersion in the cusp whereby the highest energy ions are observed at the equatorial edge of the cusp and successively lower energy ions with a low energy cutoff are observed at higher latitudes. The models have been used to demonstrate that this dispersion is consistent with the velocity filter effect and the finite extent of the reconnection region at the dayside magnetopause.

These models produce a smooth energy-latitude dispersion signature because they have relatively simple, static input conditions. Almost all in situ cusp observations show deviations from the overall smooth energy-latitude dispersion. In particular, fluctuations of the low energy cutoff of the precipitating ions have been interpreted as the result of changes in reconnection at the magnetopause [e.g., *Lockwood and Smith,* 1992]. Unfortunately, using these fluctuations as a monitor of changes in reconnection is complicated by the fact that the low energy cutoff is often difficult to observe.

The purpose of this paper is to present another method for quantifying the changes in reconnection at the magnetopause. Changes in the solar wind ion composition in the cusp are used as a proxy for changes in the precipitation velocity of the ions. Using this method, a survey is conducted of some cusp crossings of the Polar spacecraft under southward IMF conditions. The results from this survey are then related to changes in reconnection at the magnetopause.

2. SAMPLE CUSP ENCOUNTER

Figure 1 shows the Polar orbit for 15 Sept 1997. The spacecraft orbit was nearly in the noon-midnight meridian and Polar encountered the cusp at 6-7 R_E geocentric distance. Over the period of about an hour, the spacecraft moved relatively slowly from the polar cap to the equatorial edge of the cusp. The solar wind conditions were nominal during this interval. The Wind spacecraft observed a solar wind density of ~4 cm^{-3}, a bulk flow velocity of ~425 km/s and a proton thermal speed of 35 km/s. The IMF was southward and had a relatively large $+B_y$ component during the interval. (These data were corrected for the plasma convection time from Wind to Polar.)

The top two panels of Plate 1 show energy time spectrograms of the omni-directional flux of H^+ and He^{2+} observed by the Toroidal Imaging Mass Angle Spectrograph (TIMAS) [*Shelley et al.,* 1995] in the cusp. Only the last 25 minutes of the cusp traversal are shown to emphasize the composition changes discussed below (after 0400 UT, Polar was in the magnetosphere). The time resolution in Plate 1 is 4 spins (24 s) although the TIMAS instrument returns a full energy spectrum for H^+ and He^{2+} every spin (6 s). For H^+, the highest energies are observed near the equatorial edge of the cusp (at ~0400 UT) and lower energies are observed at higher latitudes. H^+ flux below 100 eV/e, especially after 0350 UT, is from the ionosphere. This energy-latitude dispersion of precipitating magnetosheath ions is consistent with magnetic reconnection at the dayside magnetopause. The dispersion is better seen in the He^{2+} spectrogram in the second panel because there is no major source of ionospheric He^{2+}. The peak fluxes for He^{2+} occur at higher energies than the peak fluxes for H^+ because the two distributions precipitate with the same velocity. The third panel shows the He^{2+}/H^+ density ratio. This ratio is initially similar to the average solar wind ratio, it then increases to values well above the solar wind ratio, and finally it decreases again near the equatorial edge of the cusp to values below the average solar wind ratio.

The change in the He^{2+}/H^+ density ratio in the cusp was first noted by *Shelley et al.* [1976]. They interpreted

this change as the result of different velocity space distributions for the source H^+ and He^{2+} populations in the magnetosheath. Their interpretation of the magnetosheath source distributions was later confirmed by H^+ and He^{2+} observations in the magnetosheath [e.g., *Peterson et al.,* 1979; *Fuselier et al.,* 1988].

Recently, a direct comparison of cusp observations and models of the magnetosheath H^+ and He^{2+} distributions has been made [*Fuselier et al.,* 1998]. (No comparison of observations has been possible to date because there have been no reported simultaneous composition measurements in the magnetosheath and in the cusp). Figure 2 is an example of this comparison of the model and observations. For the observations in Figure 2, the maximum flux for H^+ and He^{2+} in Plate 1 was converted to phase space density. These H^+ (open squares) and He^{2+} (filled circles) phase space densities are plotted in Figure 2 versus the velocity at which their respective maximum fluxes were measured. Under certain assumptions, this representation of cusp observations is directly comparable to the source distributions in the magnetosheath [*Fuselier et al.,* 1998].

The model distributions that were fit to these observations (solid lines in Figure 2) are described in detail elsewhere [*Fuselier et al.,* 1998]. Briefly, the H^+ distribution in the magnetosheath is modeled by two maxwellians representing the core component between 0 and 400 km/s and shoulder component above 400 km/s [see e.g., *Sckopke et al.,* 1983]. The He^{2+} distribution is modeled by 3 maxwellians. The first 2 represent the shell component between 0 and 500 km/s in Figure 2. Two maxwellians are used to produce the shell by subtracting a lower temperature maxwellian from a higher temperature one to produce a hole in the velocity space distribution. The third maxwellian represents the shoulder above 600 km/s [see e.g., *Fuselier and Schmidt,* 1997]. Parameters which characterize the maxwellian components are obtained from the upstream solar wind conditions measured by the Wind spacecraft. The only free parameter in the fit is the change in the thermal speed for the core H^+ component across the bow shock. This parameter fixes the core H^+ temperature below 400 km/s in Figure 2.

As seen in Figure 2, the model fits and observations compare reasonably well. For He^{2+}, the model and observations deviate from one another below about 200 km/s. This deviation is partly due to a saturation effect in the TIMAS instrument, which results in anomalously high He^{2+} count rates for high H^+ fluxes. This saturation effect produces He^{2+}/H^+ density ratios above ~15% in Plate 1.

Because the two velocity space distributions are different, the He^{2+}/H^+ phase space density (and hence the density ratio in the cusp) is a function of the velocity of

the precipitating ions. Thus, as the velocity of the precipitating ions increases in Plate 1, the He^{2+}/H^+ density ratio changes. The third solid line in Figure 2 shows the change in the He^{2+}/H^+ phase space density ratio with velocity and the scale for this ratio is on the right hand side of the figure. When the velocity of the precipitating ions is near zero, the He^{2+} and H^+ phase space densities in Figure 2 are relatively far apart, the phase space density ratio is less than 1%, and the density ratio in the cusp (for example at 0340 UT in Plate 1) is low. As the velocity of the precipitating ions increases to near 350 km/s, the He^{2+} and H^+ phase space densities approach one another in Figure 2, the phase space density ratio is over 10%, and the density ratio in the cusp (for example at 0349 UT in Plate 1) is high. Finally, as the velocity of the precipitating ions increases above 400 km/s, the He^{2+} and H^+ phase space densities become relatively far apart again, the phase space density ratio decreases, and the density ratio in the cusp (for example at 0355 UT) is low again.

Unlike the variation in the phase space density ratio from the model in Figure 2, the variation in the density ratio in the cusp is not smooth. Plate 1 shows several spikes in the density ratio, for example just before and after 0350 UT. Figure 3 shows how these spikes are related to changes in the He^{2+} flux and ultimately changes in the velocity of the precipitating ions. The top panel shows 3 contours of constant He^{2+} flux as a function of time centered on 0350 UT. The bottom panel shows the He^{2+}/H^+ density ratio. The density ratio decreases from a maximum at about 0349:10 UT to a relative minimum at 0350:20 UT and then back to a relative maximum at 0351 UT. The contours of constant flux in the upper panel of Figure 3 decrease in velocity and then increase again in concert with the changes in the density ratio.

Variations in the low energy cutoff of the precipitating ions (represented by the 5×10^4 flux contour in Figure 3) have been directly related to changes in reconnection at the magnetopause [e.g., *Lockwood and Smith*, 1992]. Thus, Figures 2 and 3 establish a direct link between changes in reconnection at the magnetopause and changes in the He^{2+}/H^+ density ratio in the cusp. With this link, the He^{2+}/H^+ density ratio becomes a proxy for the changes in the energy of the precipitating ions and ultimately the changes in reconnection at the magnetopause.

Detailed consideration of Figures 2 and 3 illustrates how this link results in quantitative determination of the changes in the velocity of the precipitating ions. The ratio of the He^{2+}/H^+ phase space densities from the model distributions in Figure 2 is used to estimate the change in the precipitating ion velocity due to the change in the density ratio observed in Figure 3. In the

lower panel of Figure 3 from 0349:10 to 0350:54 UT, the density ratio changes from over 30% to approximately 6% and then back to about 13%. The 30% density ratio is due in part to saturation of the He^{2+} signal. The value of the density ratio at this time corrected for this saturation is approximately 15%. As the density ratio changes from a maximum to a relative minimum and back to a maximum, the precipitation velocity of the ions with the maximum flux changes from about 350 km/s to about 220 km/s and then back to about 350 km/s. Thus, in about 2 minutes, the precipitating ion velocity changes a total of about 130 km/s in one direction and then back by the same amount.

Comparing this total change with the top panel of Figure 3, it is apparent that the estimated change in the precipitating ion velocity is consistent with the change in velocity of the low energy cutoff of the He^{2+} flux represented by the 5 x 10^4 flux contour. In the 2 minute time period, the low energy cutoff changes from between 160 and 200 km/s to about 90 km/s and then back to 200 km/s. The total change is between 180 and 220 km/s, compared to 260 km/s change in the velocity estimated using the model distributions in Figure 2. The uncertainties in both these estimates are approximately ±30 km/s due to the discreet energy steps in the instrument and, given the fidelity of the comparison, the two numbers compare reasonably well.

The event in Plate 1 was chosen because it had a relatively large change in the precipitating velocity that clearly demonstrated the direct link between changes in the low energy cutoff of He^{2+} and changes in the density ratio. However, the determination of the low energy cutoff is not always easy. Plate 2 shows a cusp event where the changes in the low energy cutoff are less evident. The top 2 panels in the plate are the H^+ and He^{2+} energy-time spectrograms similar to those in Plate 1. As in Plate 1, the H^+ and He^{2+} fluxes in Plate 2 show a relatively smooth energy-latitude (time) dispersion consistent with reconnection at the dayside magnetopause. The energy dispersion is reversed from Plate 1 because the spacecraft was moving toward higher latitudes in Plate 2. Although the energy-latitude dispersion is smooth, the He^{2+}/H^+ density ratio in the third panel shows considerable fluctuations. These fluctuations are correlated with changes in the He^{2+} flux, as seen in the bottom panel of Plate 2. Changes in the H^+ flux and in particular in the low energy cutoff of the flux are much less evident in the top panel.

3. SURVEY OF SELECTED SOUTHWARD IMF EVENTS

Nine cusp events including those in Plates 1 and 2 were chosen to survey the changes in the density ratio

and their relation to changes in the velocity of the pre-
cipitating ions and changes in reconnection at the mag-
netopause. All 9 events exhibited good energy-latitude
dispersion as in Plates 1 and 2. All events occurred
when the IMF was southward as observed by the Wind
spacecraft. Most significantly, all events exhibited fluc-
tuations in the density ratio similar to the fluctuations in
Plates 1 and 2.

For each event, the solar wind conditions from the
Wind spacecraft were used to model the magnetosheath
distributions as in Figure 2. From these model distribu-
tions, the change in the He^{2+}/H^+ density ratio was di-
rectly related to the change in the velocity of the pre-
cipitating ions as in the discussion of Figures 2 and 3 in
the previous section. For all events, the period between
maxima in the density ratio was measured. For exam-
ple, in the third panel of Figure 2, there are 4 peaks in
the He^{2+}/H^+ density ratio at about 0345, 0347, 0349,
and 0351 UT. For each of these oscillations in the den-
sity ratio, the total velocity change was computed using
the model distributions. For example, the oscillation
isolated in Figure 3 had a total velocity change of the
precipitating ions of 260 km/s (as discussed in the pre-
vious section). This total change consisted of a 130
km/s excursion to lower velocities followed by a 130
km/s excursion back to higher velocities within a period
of about 2 minutes.

Figure 4 shows the total velocity change of the pre-
cipitating ions as a function of the period between peaks
in the density ratio. There is considerable scatter in the
points and no correlation is evident. The average period
was about 2 minutes and the total velocity change was
130 km/s. It is significant that the change in the veloc-
ity of the precipitating ions in Figure 3 was considerably
larger than this average. This made it a good choice for
illustrating how the density ratio change and the veloc-
ity of the precipitating ions are related.

Figure 5 shows the maximum velocity of the precipi-
tating ions (defined as the velocity where the density ra-
tio was maximum) as a function of the period between
maxima in the density ratio. This plot shows that the
longer period oscillations in the density ratio occur
when the maximum flux is at lower velocities. An ex-
ample of this trend is seen in Plate 2. The last two os-
cillations in the density ratio (from 1657 to 1702 UT)
occur 5 minutes apart when the precipitating ion flux is
at lower energies. Nearer to the equatorial edge of the
cusp, where the energies are higher, the periods are of
the order of 2 minutes. This may indicate that the cause
for precipitating ion velocity changes and reconnection
changes are different for plasma in the traditional
"cusp" than for plasma in the traditional "mantle". This
is a subject for future study.

4. INTERPRETATION

As stated in the introduction, the goal of this study is to relate the changes in the cusp to changes in reconnection at the magnetopause. In the previous section, changes in low energy cutoff of the precipitating ions were related to changes in the density ratio. In Figure 4, the average period between oscillations in the precipitating ion flux was about 2 minutes and the average total change in the velocity of the precipitating ions was 130 km/s. Thus, the low energy cutoff velocity of the precipitating ions changes by about 65 km/s in about 1 minute. In this section, these average changes are related to possible changes in magnetopause reconnection.

In the simple interpretation of the cusp as a velocity filter, a change in the velocity of the precipitating ions occurs because the time-of-flight of the ions that reach the spacecraft has changed. This change can occur by moving the reconnection line, changing the convection velocity of the field line, or changing the rate of reconnection at the magnetopause. Any combination of these changes could also occur, but it is important to estimate the magnitude of the required changes for each process individually.

The basic equation for the time of flight of an ion from the reconnection site to the spacecraft is:

$$V_{\|i} = L_i / t \tag{1}$$

where L is the length of the magnetic field line (~10 R_E) and $V_\|$ is the velocity of the ion parallel to the magnetic field.

Moving the Reconnection Line

By moving the reconnection line along the magnetopause, L in (1) is changed. If the time is constant, then the parallel velocity of the precipitating ions must change. For L_1 ~10 R_E (a typical distance from the subsolar point to the Polar spacecraft in the cusp), $V_\|$ ~ 300 km/s (from Figure 5), and the change in $V_\|$ ~65 km/s (from half of the average in Figure 4), L_2 ~ 12 R_E. Thus, to account for the average changes in the velocity of the precipitating ions in the cusp, the reconnection line must move 2 R_E (poleward or equatorward along the magnetopause) and then return 2 R_E to near its original position. These are large changes in the position of the X-line that require accelerations of the X-line of the order of 10 km/s^2. The consequences of such accelerations would be very obvious in the in situ observations at the magnetopause. The fact that changes in the location of the reconnection site during multiple magnetopause crossings are not typically observed suggests

that this is not the dominant means whereby reconnection conditions are changed on 1 minute time scales.

Changing the Field Line Convection Velocity

A reconnected field line convects with the deHofmann-Teller velocity at the magnetopause. If this velocity is increased or decreased, then the parallel velocity of the precipitating ions must increase or decrease by the same amount to keep the time of flight of the ions from the reconnection site to the spacecraft constant. A 65 km/s increase in the parallel velocity from 300 to 365 km/s (from one half the average total change in $V_{\parallel}$ in Figure 4 and the average velocity of the precipitating ions in Figure 5) represents about a 20% change in the parallel velocity of the precipitating ions. Thus, in about 1 minute, the deHoffmann-Teller velocity changes by about 65 km/s. The deHoffmann-Teller velocity has been measured for selected in situ observations of magnetopause crossings [e.g., *Sonnerup et al.,* 1990]. The existence of this velocity is a necessary condition for reconnection at the magnetopause. Under certain assumptions, the bulk flow of the plasma on either side of the open magnetopause is at the local Alfven velocity in the frame of reference moving with the deHoffmann-Teller velocity. In a few special cases, it was found that there was better agreement between the observed velocities and the local Alfven speed if the deHoffmann-Teller velocity was not constant. In particular, accelerations of the order of 1 km/s^2 tangential to the magnetopause were needed to achieve better agreement between theory and observation [*Sonnerup et al.,* 1990]. Typical spacecraft crossings of the magnetopause take about 1 minute and deHoffmann-Teller velocities are typically of the order of 300 km/s. Thus, the ~1 km/s^2 acceleration of the deHoffmann-Teller frame represents about a 20% change in the deHoffmann-Teller velocity during a magnetopause crossing. Although very few magnetopause crossings have been investigated in such detail, the inferred order of magnitude of the acceleration is consistent with the changes in the cusp ion precipitation in Figure 4.

Changing the Reconnection Rate

If the inflow of magnetic field lines into the reconnection region increases, then the magnetopause moves inward (erosion) and equatorial edge of the cusp moves equatorward. For a near stationary spacecraft such as Polar in the high latitude cusp, this would cause the energy of the precipitating ions that arrive at the spacecraft to decrease. If the tangential electric field and the normal component of the magnetic field at the magnetopause change by equal amounts, then the deHoffmann-Teller velocity remains constant while the recon-

nection rate changes. Also, the position of the X-line on the magnetopause does not change. Thus, while the field line convection velocity and the X-line position do not change, the movement of the equatorial edge of the cusp to lower latitudes through magnetopause erosion effectively changes the position of the spacecraft in the cusp. This process of changing the reconnection rate without changing the field line convection velocity has been suggested previously [e.g., *Lockwood and Smith,* 1992].

Since this change in the reconnection rate is linearly related to the change in the parallel convection velocity required to reach the spacecraft, the ~20% change in the parallel convection velocity represents a 20% change in the reconnection rate. As stated in the introduction, the reconnection rate is very difficult to measure with in situ observations at the magnetopause. Thus, it is difficult to determine from independent measurements at the magnetopause if the rate varies continuously by about ±20% or more. The only direct signature of this variation is the movement of the magnetopause and the simultaneous shifting of the cusp to higher or lower latitudes. Recent simultaneous observations from the ground and at the magnetopause indicate that this certainly occurs [*Mende et al.,* 1998]. Once again, there are few simultaneous observations of the magnetopause and cusp positions so there is only enough information to conclude that erosion may be a mechanism for producing the changes in the precipitation velocity in Figure 4.

5. CONCLUSIONS

In this paper, an additional method for quantitative investigation of short term (~minute) variations in reconnection at the magnetopause was presented. Previously, these changes were investigated by directly observing changes in the low energy cutoff velocity of the precipitating ions in the cusp. Here, the change in the He^{2+}/H^+ density ratio was introduced as a proxy for this change in the cutoff velocity.

Oscillations in the He^{2+}/H^+ density ratio were observed in all events surveyed here. The average change in the precipitating ion velocities deduced from these oscillations was about 130 km/s (65 km/s in one direction and then 65 km/s in the other) over an average period of 2 minutes. Such changes maybe due to movement of the reconnection line along (tangential to) the magnetopause, changes in the deHoffmann-Teller velocity at the magnetopause, and/or changes in the reconnection rate. The amplitude of the changes in the velocity of the precipitating ions in the cusp is large enough to rule out movement of the reconnection line along the magnetopause as the prime reason for the

changes. This amplitude is consistent with ~20% changes in either the deHoffmann-Teller velocity or the reconnection rate or some combination of both possibilities. Changes in the deHoffmann-Teller velocity of that magnitude have been observed at the magnetopause for some magnetopause crossings. The signature of a 20% change in the reconnection rate would be a simultaneous inward (outward) motion of the magnetopause and equatorward (poleward) motion of the cusp. Such simultaneous motion has been observed. Distinguishing between these two possibilities requires simultaneous observations at the magnetopause and in the cusp.

REFERENCES

Dungey, J. W., Interplanetary field and the auroral zones, *Phys. Rev. Lett., 6*, 47, 1961.

Fuselier, S. A., E. G. Shelley, and D. M. Klumpar, AMPTE/CCE observations of shell-like He^{2+} and O^{6+} distributions in the magnetosheath, *Geophys. Res. Lett., 15*, 1333, 1988.

Fuselier, S. A., and W. K. H. Schmidt, Solar wind He^{2+} ring beam distributions downstream from the Earth's bow shock, *J. Geophys. Res., 102,* 11,273, 1997.

Fuselier, S. A., E. G. Shelley, W. K. Peterson, and O. W. Lennartsson, Solar wind He^{2+} and H^+ distributions in the cusp for southward IMF, in Polar Cap Boundary Phenomena, ed. J. Moen et al., p. 63, Kluwer Academic, Netherlands, 1998.

Lockwood, M. and M. F. Smith, The variation of reconnection rate at the dayside magnetopause and cups ion precipitation, *J. Geophys. Res., 97*, 14,841, 1992.

Mende, S. B., D. M. Klumpar, S. A. Fuselier, and B. J. Anderson, Dayside auroral dynamics: South Pole - AMPTE/CCE observations, *J. Geophys. Res., 103*, 6891, 1998.

Newell, P., and C.-I. Meng, Mapping the dayside ionosphere to the magnetosphere according to particle precipitation characteristics, *Geophys. Res., Lett., 19*, 609, 1992.

Onsager, T. G., C. A. Kletzing, J. B. Austin, and H. MacKiernan, Model of magnetosheath plasma in the magnetosphere: Cusp and mantle particles at low altitudes, *Geophys. Res. Lett., 20*, 479, 1993.

Peterson, W. K., E. G. Shelley, R. D. Sharp, R. G. Johnson J. Geiss, and H. Rosenbauer, H^+ and He^{++} in the dawnside magnetosheath, *Geophys. Res. Lett., 6*, 667, 1979.

Phan, T.-D., G. Paschmann, B. U. Ö. Sonnerup, Low latitude dayside magnetopause and boundary layer for high magnetic shear 2. Occurrence of magnetic reconnection, *J. Geophys. Res., 101*, 7817, 1996.

Reiff, P., T. H. Hill, and J. L. Burch, Solar wind injection at the dayside magnetospheric cusp, *J. Geophys. Res., 82*, 479, 1977.

Rosenbauer, H., H. Grünwaldt, M. D. Montgomery, G. Paschmann, and N. Sckopke, HEOS 2 plasma observations in the distant polar magnetosphere: The plasma mantle, *J. Geophys. Res., 80*, 2723, 1975.

Sckopke, N., G. Paschmann, S. J. Bame, J. T. Gosling, and C. T. Russell, Evolution of ion distributions across a nearly perpendicular bow shock: Specularly and non-specularly reflected-gyrating ions, *J. Geophys. Res., 88*, 6,121, 1983.

Shelley, E. G., R. D. Sharp, and R. G. Johnson, He^{++} and H^{+} flux measurements in the dayside cusp: Estimates of convection electric field, *J. Geophys. Res., 81*, 2363, 1976.

Shelley, E. G., et al., The toroidal imaging mass-angle spectrograph (TIMAS) for the Polar mission, in *The Global Geospace Mission*, ed. C. T. Russell, p 497 Kluwer Academic, Netherlands, 1995.

Sonnerup, B. U. Ö., and B. G. Ledley, Electromagnetic structure of the magnetopause and boundary layer, *in Magnetospheric Boundary Layers*, B. Battrick, ed., p. 401, ESA SP 148, European Space Agency, Paris, 1979.

Sonnerup, B. U. Ö., G. Paschmann, I. Papamastorakis, N. Sckopke, G. Haerendel, S. J. Bame, J. R. Asbridge, J. T. Gosling, and C. T. Russell, Evidence for magnetic field reconnection at the Earth's magnetopause, *J. Geophys. Res., 86*, 10,049, 1981.

Sonnerup, B. U. Ö., I. Papamastorakis, G. Paschmann, and H. Lühr, The magnetopause for large magnetic shear: Analysis of convection electric fields from AMPTE/IRM, *J. Geophys. Res., 95*, 10,541, 1990.

Stephen A. Fuselier and Karlheinz J. Trattner, Dept H1-11 Bldg 255, Lockheed Martin Advanced Technology Center, 3251 Hanover St., Palo Alto, CA 94304, USA.

Figure 1. Polar orbit for 15 September 1997. The spacecraft spent almost an hour in the cusp, moving from the poleward edge to the equatorward edge.

Plate 1. Omni-directional flux of H^+ and He^{2+} and the He^{2+}/H^+ density ratio for a representative traversal of the cusp. H^+ (above ~100 eV/e) and He^{2+} show a characteristic energy-latitude dispersion from high to low energies as the spacecraft moves from high to low latitudes. The He^{2+}/H^+ density ratio changes from below the nominal solar wind ratio to well above it and then back to below it as the spacecraft traverses the cusp.

Figure 2. Maximum H^+ and He^{2+} flux from 0342-0359 UT in Plate 1 versus the velocity of the maximum flux. Under certain assumptions, this is directly comparable to the source distributions in the magnetosheath (represented by the model fits). The ratio of the phase space densities has the same profile with velocity as the density ratio in Plate 1.

Figure 3. Contours of constant flux and the He^{2+}/H^+ density versus time for part of the event in Plate 1. Changes in the low velocity cutoff of the flux (represented by the 5 x 10 4 flux contour) are directly related to changes in the density ratio.

Plate 2. Omni-directional flux of H^+ and He^{2+}, He^{2+}/H^+ density ratio, and the maximum flux for H^+ and He^{2+} for another cusp traversal. The energy-latitude dispersion is similar to Plate 1 but reversed in time because the spacecraft is moving from equatorward to poleward. Oscillations in the He^{2+}/H^+ density ratio are clearly evident but correlation with changes in the lower energy cutoff in H^+ are not evident at all.

Figure 4. Total velocity change of the precipitating ions versus the period between these changes (determined by the period between successive peaks in the He^{2+}/H^+ density ratio). The average period between these velocity changes from all events was 2 minutes and the average total velocity change was 130 km/s.

Figure 5. Maximum velocity (defined as the velocity at which the He^{2+}/H^+ density ratio is maximum) versus the period. Longer period oscillations in the precipitating ion velocity occur when the maximum velocity is low. This may be an indication that there are longer period changes in reconnection for field lines connected to the mantle.

Figure 1. Polar orbit for 15 September 1997. The spacecraft spent almost an hour in the cusp, moving from the poleward edge to the equatorward edge.

Plate 1. Omni-directional flux of H^+ and He^{2+} and the He^{2+}/H^+ density ratio for a representative traversal of the cusp. H^+ (above ~100 eV/e) and He^{2+} show a characteristic energy-latitude dispersion from high to low energies as the spacecraft moves from high to low latitudes. The He^{2+}/H^+ density ratio changes from below the nominal solar wind ratio to well above it and then back to below it as the spacecraft traverses the cusp.

Figure 2. Maximum H^+ and He^{2+} flux from 0342-0359 UT in Plate 1 versus the velocity of the maximum flux. Under certain assumptions, this is directly comparable to the source distributions in the magnetosheath (represented by the model fits). The ratio of the phase space densities has the same profile with velocity as the density ratio in Plate 1.

Figure 3. Contours of constant flux and the He^{2+}/H^+ density versus time for part of the event in Plate 1. Changes in the low velocity cutoff of the flux (represented by the 5 x 10 4 flux contour) are directly related to changes in the density ratio.

Plate 2. Omni-directional flux of H^+ and He^{2+}, He^{2+}/H^+ density ratio, and the maximum flux for H^+ and He^{2+} for another cusp traversal. The energy-latitude dispersion is similar to Plate 1 but reversed in time because the spacecraft is moving from equatorward to poleward. Oscillations in the He^{2+}/H^+ density ratio are clearly evident but correlation with changes in the lower energy cutoff in H^+ are not evident at all.

Figure 4. Total velocity change of the precipitating ions versus the period between these changes (determined by the period between successive peaks in the He^{2+}/H^+ density ratio). The average period between these velocity changes from all events was 2 minutes and the average total velocity change was 130 km/s.

Figure 5. Maximum velocity (defined as the velocity at which the He^{2+}/H^+ density ratio is maximum) versus the period. Longer period oscillations in the precipitating ion velocity occur when the maximum velocity is low. This may be an indication that there are longer period changes in reconnection for field lines connected to the mantle.

FUSELIER AND TRATTNER: CUSP ION COMPOSITION AND NON-STEADY RECONNECTION
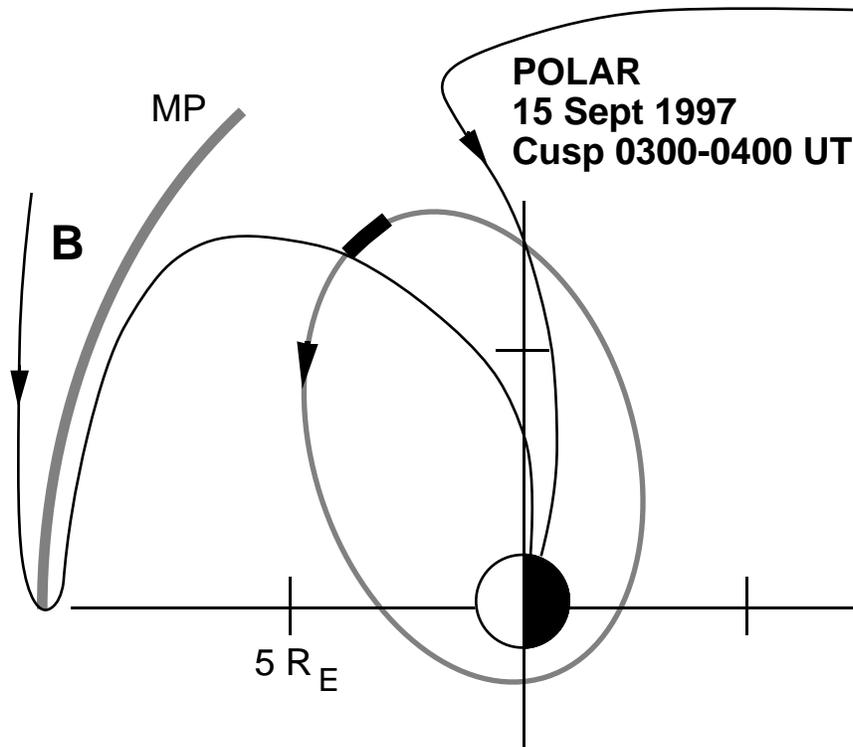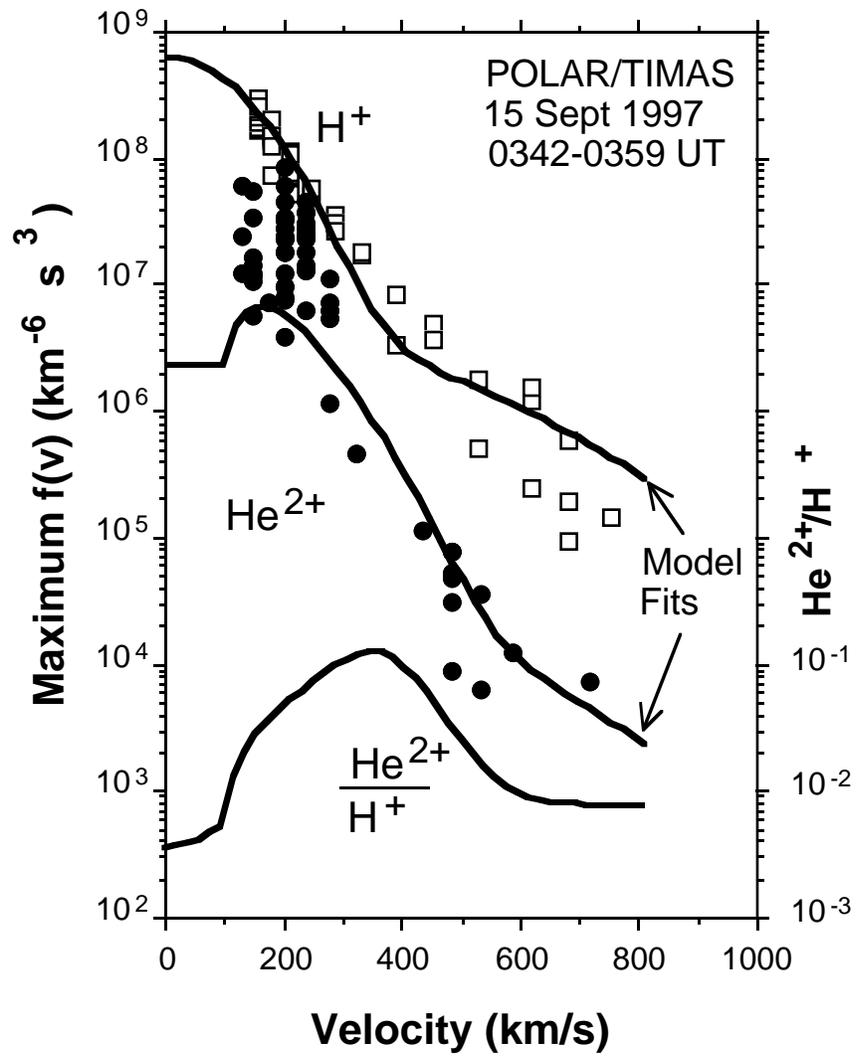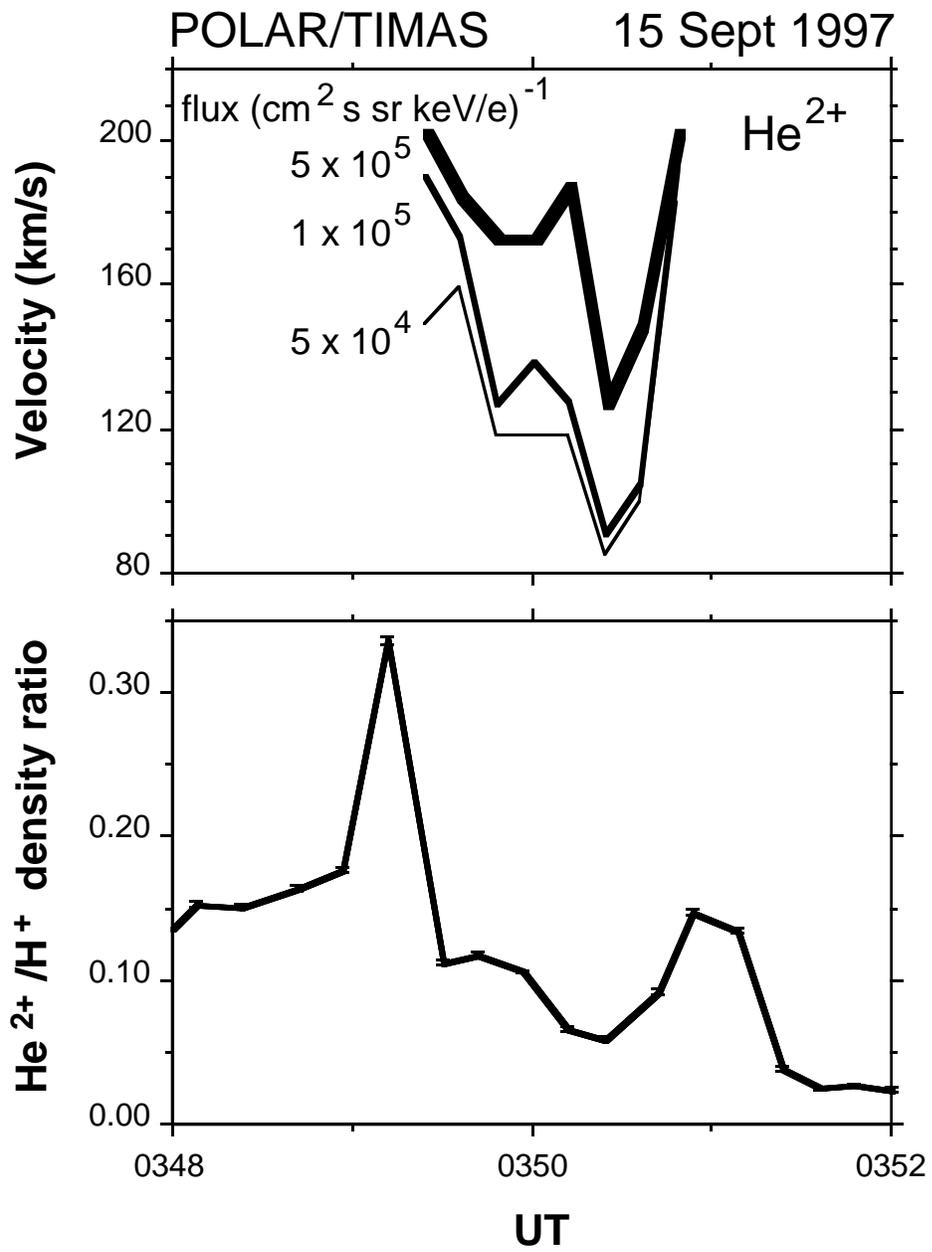
MP

B

**POLAR
15 Sept 1997
Cusp 0300-0400 UT**

5 R$_E$

Figure 1

Figure 2

Figure 3

Figure 4

Figure 5

POLAR/TIMAS   15 Sept 1997

H$^+$ (keV/e)

10.0

1.0

0.1

He^{2+} (keV/e)

10.0

1.0

0.1

He^{2+}/H$^+$density

0.30

0.20

0.10

0.00

POLAR/TIMAS

Nominal
Solar Wind

10^8

10^7

10^6

10^5

10^4

10^3

Flux (1./cm^2 sr s keV/e)

UT	0335	0400
R	6.8	6.4
MLT	1247	1301
MLat	53.5	48.6

Plate 1

Maximum f(v) (km^{-6} s^{3})

POLAR/TIMAS   24 April 1996

H$^+$ (keV/e)

10.0

1.0

0.1

He^{2+} (keV/e)

10.0

1.0

0.1

10^8

10^7

10^6

10^5

10^4

10^3

Flux (1./cm^2 sr s KeV/e)

0.12

0.08

0.04

0.00

He^{2+}/H$^+$density

POLAR/TIMAS

WIND/SWE

Maximum Flux (x 10^7)

6

4

2

0

H$^+$

He^{2+} x10

He^{2+}/H

UT	1645	1710
R	4.6	5.2
MLT	1158	1159
MLat	59.9	66.9

0   200   400   600   800   1000

Plate 2

Velocity (km/s)